Journal of Applied Sciences and Nanotechnology

Journal homepage: https://jasn.uotechnology.edu.iq/

A Review on the Kesterite Cu_2ZnSnS_4 Prepared by Solvo/ Hydrothermal Method

[1,2]Nabaa H. Allawi*, [1]Selma M. H. Al-Jawad

[1]Department of Applied Sciences, University of Technology – Iraq

[2]Center of Solar Energy Research, Ministry of Science and Technology – Iraq

Article information

Article history:
Received: September, 01, 2023
Accepted: January, 22, 2024
Available online: March, 10, 2024

Keywords:
Solvothermal method,
Hydrothermal method,
Kesterite CZTS

***Corresponding Author:**
Nabaa H. Allawi
as.18.20@grad.uotechnology.edu.iq

Abstract

Cu_2ZnSnS_4 (CZTS) is a promising material for use in solar cells. The distinctive characteristics of this substance include its abundance on earth, low cost, non-toxicity, high absorption coefficient, p-type conductivity, and ideal band gap. CZTS has a stannite (ST) and kesterite (KS) crystal structure. Kesterite has more excellent thermodynamic stability compared to stannite. Consequently, CZTS most frequently occurs in this era. Sputtering, thermal evaporation, pulsed laser deposition, spray pyrolysis, chemical vapour deposition, spin coating, electrodeposition, SILAR, sol-gel, solvothermal, and hydrothermal are among the several processes employed for the production of CZTS thin films. The solvothermal and hydrothermal processes are commonly used to produce high-quality nanocrystals with unique morphology, crystallographic structure, and cost-efficient production.Furthermore, the solvothermal and hydrothermal techniques were employed to produce various categories of photovoltaic devices utilising CZTS, including photoelectrochemical cells, dye-sensitised solar cells, perovskite solar cells, and heterojunction solar cells. In addition, the solvothermal and hydrothermal methods were used to fabricate other types of photovoltaic devices using CZTS, such as photoelectrochemical cells, dye-sensitised solar cells, perovskite solar cells, and heterojunction solar cells. Additionally, it provides a survey on using CZTS in photovoltaic applications, which are produced by hydrothermal and solvothermal techniques. The article also addresses the obstacles encountered in implementing these applications. Lastly, it provides the opportunity to identify remedies for these difficulties.

DOI: 10.53293/jasn.2024.7099.1244, Department of Applied Sciences, University of Technology - Iraq.

1. Introduction

Because of the anticipated increase in global energy consumption, humanity must be able to generate 30 TW of electricity (1 TW = 10^{12} W) by 2050 without emitting carbon dioxide. Solar photovoltaic (PV) offers the potential to supply the world's energy requirements in the future [1]. The two most common wafer technologies used to produce photovoltaic (PV) cells are crystalline silicon and polycrystalline silicon, which account for more than

80% of the market. Thicker coatings are necessary for these technologies' indirect bandgap absorber material to maximize the amount of solar energy absorbed. The need for perfect crystals in high-efficiency solar modules drives up the cost of PV equipment. As a result, thin-film PV technologies have become increasingly popular as an alternative to traditional PV technologies in modern PV development [2]. Recent reports indicate that thin-film PV systems utilizing direct bandgap materials, such as cadmium telluride, copper indium diselenide, and copper indium gallium diselenide, can achieve module conversion efficiencies ranging from 16.5-21.5 percent [2-4]. The presence of hazardous Cd and Te and the expensive cost of Ga and In restricts the potential for further developments in solar cells [5-7]. Therefore, researchers are looking into cheaper, more efficient, and safer alternatives for solar cell construction. The discovery that Cu_2ZnSnS_4 (CZTS) and CIGS share structural similarities piqued the interest of scientists. As well as the earth's abundance, low cost, non-toxicity, perfect band gap, high absorption coefficient, and P-type conductivity of CZTS are additional special features [8]. Because of these features, it is perfect for use in solar cells. The electrical and optical properties greatly affect solar cell performance, mainly regulated by the absorber material's composition and crystal structure [9].

There are a variety of physical and chemical techniques that can be used to prepare CZTS. Chemical techniques offer greater convenience and cost-effectiveness in comparison to physical processes. Chemical procedures include vapor-based and wet chemical (solution-based) methods. The wet chemical approach is more cost-effective compared to chemical vapor-based technologies. The material is synthesized using a variety of processes, including spray pyrolysis, electrodeposition, spin coating, anodization, hydrothermal, solvothermal, sol-gel, co-precipitation, and combustion. Typically, these approaches entail a reaction process that may or may not involve thermal aid [10]. Chemical methods offer more ease in controlling deposition parameters compared to physical approaches. Techniques such as sequential ionic layer adsorption and reaction (SILAR), spin coating, solvo/hydrothermal, electrodeposition, spray pyrolysis, and chemical bath deposition (CBD), anodization are employed to produce microcrystalline films onto the substrate directly. Meanwhile, various techniques such as hydrothermal, sol-gel, co-precipitation, and combustion are employed to synthesize nanoparticles of the desired material [11]. These nanoparticles are then mixed with a suitable solvent to produce an ink or paste and subsequently subjected to heat treatment. Solventothermal and hydrothermal approaches have also gained significant popularity due to their ability to produce high-quality nanocrystals with distinctive shapes and crystal structures. Also, it offers several morphologies [12-15].

Several exhaustive reviews published on CZTS were prepared using sputtering, spray pyrolysis, and pulsed laser deposition methods [16-18]. However, there is no comprehensive review of the preparation of CZTS by solvothermal and hydrothermal methods. This review primarily concentrates on the fundamental aspects of CZTS growth by utilizing the solvo/hydrothermal process. We provide a concise examination of the factors that impact the structure, shape, and optical characteristics of CZTS produced using hydrothermal and solvotherma. Finally; we summaries the photovoltaic devices fabricated based on the CZTS compound and the challenges that affected these devices.

2. Structure of Cu_2ZnSnS_4

Due to its distinctive features, the scientific community has recently been more enthusiastic about the (CZTS). I2-II-IV-IV4 quaternary semiconductor compound was developed by replacing In atoms in $CuInS_2$ (CIS) chalcopyrite ternary compound with Zn and Sn atoms, respectively. The crystal structure of CZTS is composed chiefly of stannite (ST) and kesterite (KS).As can be seen in Fig. 1, the crystal structures of the CZTS compounds ST and KS have been determined. The only difference between the two structures is how the Cu and Zn atoms are arranged [18]. The KS has a lower formation energy; the KS and ST bond energies are identical (3 MeV/atom). Kesterite is thermodynamically more stable than stannite. Hence, it is the phase in which CZTS typically occurs. CZTS and CIGS share similar carrier concentrations and absorption coefficients. CZTS also has poor qualities like carrier lifetime. This short carrier lifetime could be caused by recombination at grain boundaries or a large concentration of functional defects [20]. CZTS has a direct band-gap energy of 1.4 to 1.5 eV, p-type conductivity, and uses non-toxic and abundant earth elements, all of which may stimulate its widespread adoption as an inexpensive, non-hazardous, environmentally secure, and abundant absorber layer in thin film solar cells (TFSCs) [21]. Table (1) shows the physical properties of the CZTS compound [17, 22].

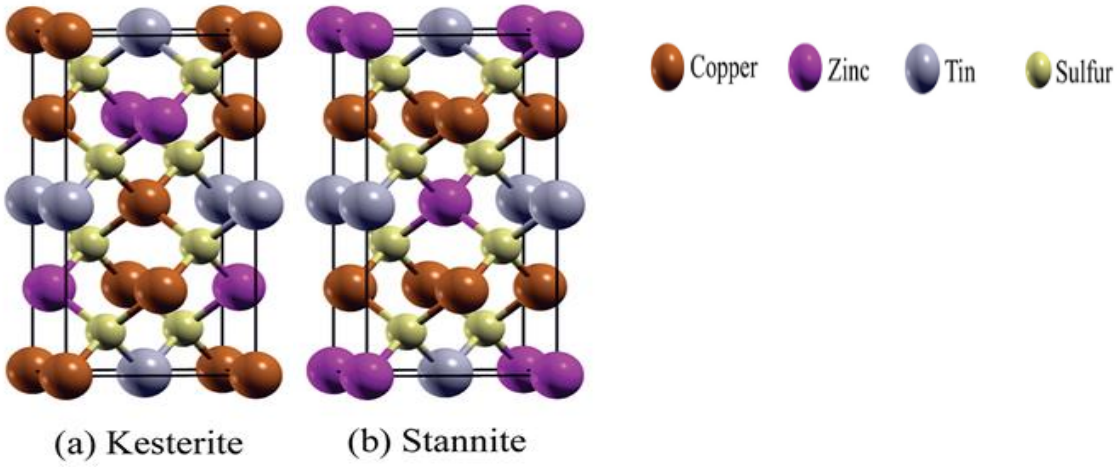

Figure 1: kesterite and stannite structures of CZTS compound [19].

Table 1: The properties of the CZTS compound [17, 22].

Parameters	Properties
Chemical formula	Cu_2ZnSnS_4
Molecular weight	439.47 g/mole
Density	4.56 g/cm^3
Melting point	990 C^0
Solubility in water	Insoluble
Solubility	Soluble in acids and alkalis
Thermal conductivity for single crystalline	5.1 Wm^{-1} K^{-1}
Thermal conductivity for poly crystalline	4.0 Wm^{-1} K^{-1}
Lattice constant a	5.42 A
Lattice constant c	10.848 A
Conductivity	P-type

3. Solvo/hydrothermal Method

A solvo/hydrothermal reaction is any chemical reaction that occurs in the presence of water or an aqueous organic solvent and mineralizes at high pressures and temperatures to dissolve and recrystallize generally insoluble materials [23]. These methods have been widely used in waste treatment [24], synthesizing traditional and modern materials and imitating geothermal and biohydrothermal processes. As a result, the study of solvothermal and hydrothermal processes is the initial stage in creating new materials such as TiO_2, CdS, CuS, ZnS, TiO_2:Mn, TiO_2:Ni, Bi_2MO_6 and CdS: Mn [25-31]. Three features distinguish a hydrothermal system: it accelerates the rate of hydrolysis, increases the rate of interaction between complex ions, and significantly modifies the redox potential of the reactants. Typically, there are two types of elementary chemical reactions. An example of such a reaction is the ionic reaction, which involves the exchange of ions in inorganic substances and can be rapidly accomplished at ambient temperature. The free radical reaction is another example, as is the explosive decomposition of organic molecules [32]. Understanding the correlation between water pressure and temperature helps enhance understanding of hydrothermal synthesis [33, 34]. The relationship between water pressure and temperature for different fill degrees is seen in Fig. 2. The degree of fill and pressure for a normal solvo/hydrothermal synthesis experiments are typically between (50%-80%) and (200-3000) bar, respectively. The reaction solution's filling affects the pressure under hydrothermal conditions [34, 35]. Occasionally, the reaction pace can be enhanced when the solvent or a constituent of the reactants alters the chemical and physical characteristics of both the reactants and the resulting products [34]. In summary, under high temperature and hydrothermal pressure conditions, water may function as water serves as reaction media for hydrothermal synthesis. In contrast, other organic solvents are used in solvothermal synthesis. In solvothermal synthesis, the organic solvent serves as both a reaction media and a solvent-reactant complex that dissolves or partially dissolves the reactants, affecting the rates of the chemical reactions [23, 33]. The organic solvent might potentially influence the concentration and condition of the reactive

active species, hence modifying the reaction's progression. Before selecting an organic molecule as a solvent, evaluating its role in the synthesis process is essential. The solvothermal method has utilized a variety of alcohols. The relationship between the organic pressure and the temperature of various organic solvents is illustrated visually in Figs. (3 & 4) is a representation of autoclaves made of stainless steel and Teflon that have components on the inside. The hydro/solvothermal technique for crystal growth has benefits over other approaches, such as forming unstable crystal phases close to the melting point. The hydrothermal method also permits the hydro/solvothermal development of substances with high vapor pressures near their melting points. The process is also well suited for the composition-controlled development of massive, high-quality crystals [35].

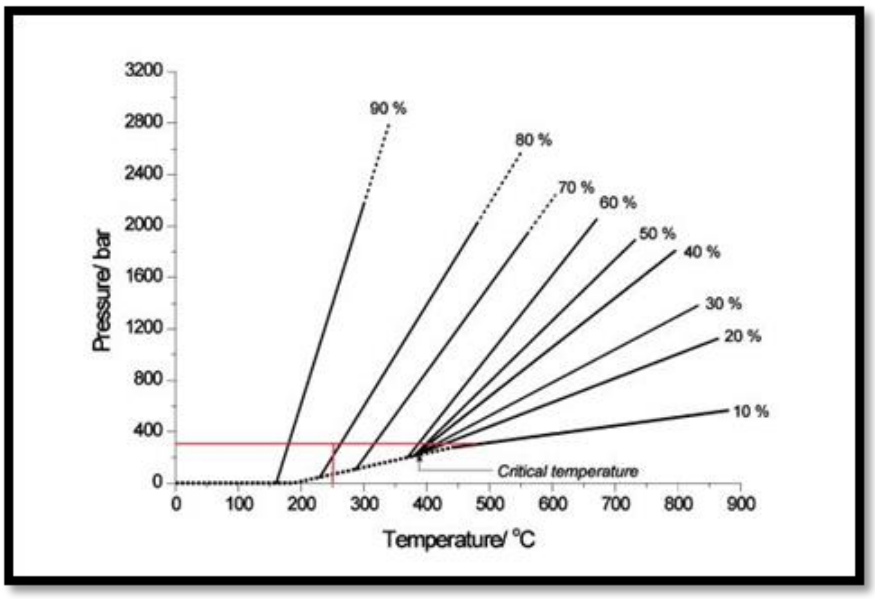

Figure 2: The correlation between water temperature and pressure at various fill levels [34].

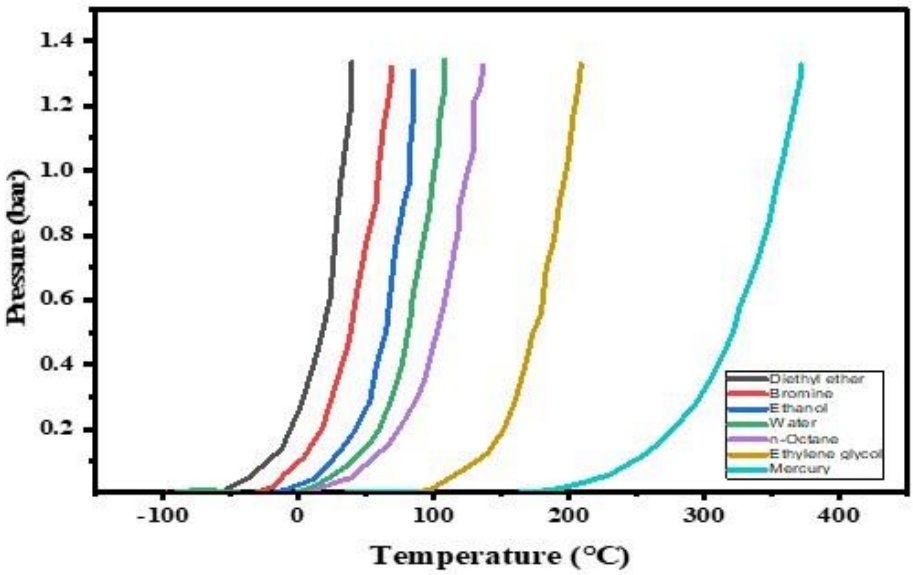

Figure 3: The relationship between temperature and pressure for several organic solvents [36].

Figure 4: Image of Teflon lined stainless steel autoclave with inner components [37].

3.1. Advantages of Hydrothermal and Solvothermal Methods

There are several advantage of hydrothermal and solvothermal methods such as Oxides, hydroxides, chlorides, acetates, and nitrates are used as inexpensive precursor chemicals in the process. Also, low-temperature hydrothermal synthesis may produce various effects even at temperatures below 300°C. Stable precursors may be destroyed under pressure at a comparatively low temperature, preventing the significant agglomeration that solid-state processes often bring about at high sintering temperatures. The powders made during solvo/hydrothermal synthesis are notably purer than the components used in the process. Growing crystals or crystallites have a natural tendency to avoid absorbing impurities from their surroundings during the hydrothermal crystallization process post-sintering or calcination processes are seldom necessary for powders/film generated using the solvo/hydrothermal technique. Because it employs a closed system that allows for the retrieval and reuse of numerous different components, synthesis is an environmentally friendly process [34, 36, 38].

3.2. Disadvantages of Solvo/ hydrothermal Method

The disadvantages of solvo/ hydrothermal method are: a major drawback of the solvo/hydrothermal synthesis technique is the rather long procedure, which can take anything from four to seventy-two hours. One disadvantage of hydrothermal and solvothermal synthesis is the energy consumption it entails due to the temperatures and pressures normally needed. Extreme and corrosive conditions, including high pressures, temperatures, and reactive solvents, are common for hydrothermal and solvothermal reactions to take place. Corrosion of the reaction vessels or degradation of the produced materials are some of the potential outcomes of these conditions. These corrosive and reactive situations necessitate using specialized materials and equipment that can endure them. Finally, achieving reproducibility and standardization can be challenging in hydrothermal and solvothermal synthesis. Small variations in parameters for reactions, such as pressure, concentration, temperature, and reaction time, can significantly affect the resulting materials. Ensuring consistent and reliable synthesis conditions can be demanding and require careful optimization [34, 36, 39].

4. Growth Mechanism

CZTS compound may be grown by solvo/hydrothermal as particles or as a film.

4.1. Growth Mechanism of Particles

Crystallization directly from solutions is a procedure used to synthesize materials using hydrothermal/ solvothermal processes. Nucleation and crystal growth are the two usual steps to synthesize materials using hydrothermal and solvothermal processes. By adjusting processing variables like pH, reactant concentrations, temperature, and additives, it is feasible that the final product can be made with the specified particle sizes and shapes. Improve the size and shape regulation achieved by adjusting the process parameters. Supersaturation determines the overall rates of nucleation and growth. Supersaturation is the difference between the saturation concentration and the accurate concentration of a species in a solution [40]. Nucleation occurs when the solute's solubility in the solution surpasses its limit or when it is supersaturated. Even though it is difficult to estimate the precise reaction equilibrium due to the large number of species involved, various thermodynamic models have been created to evaluate the solubility of the species in hydrothermal/solvothermal systems, particularly in aqueous solutions. For instance, Shock and colleagues have revised the Helgeson-Kirkham-Flowers (HKF) model [41, 42].

Hundreds of inorganic compounds' aqueous solution solubilities have been predicted using the HKF model across a large temperature and pressure range (25-1,000 C, 1-5000 bar). The solvent's characteristics, especially its density and dielectric constant, significantly impact the solubility of species in the solution. The process is irreversible, and the solute forms crystal aggregates that can grow to a macroscopic scale. After nucleation, the crystals engage in many processes that lead to their growth, such as incorporating growth units from the surrounding solution into the existing crystal structures. There is no difference in composition between these growth units and crystal entities, and the structures can be the same or different. The various processes involved can be simplified into four general categories: surface unit mobility, surface unit attachment, growth site attachment, and solution unit movement. The crystal growth of particles prepared by a cuhydrothermal/solvothermal method is depicted in Fig. 5 [42].

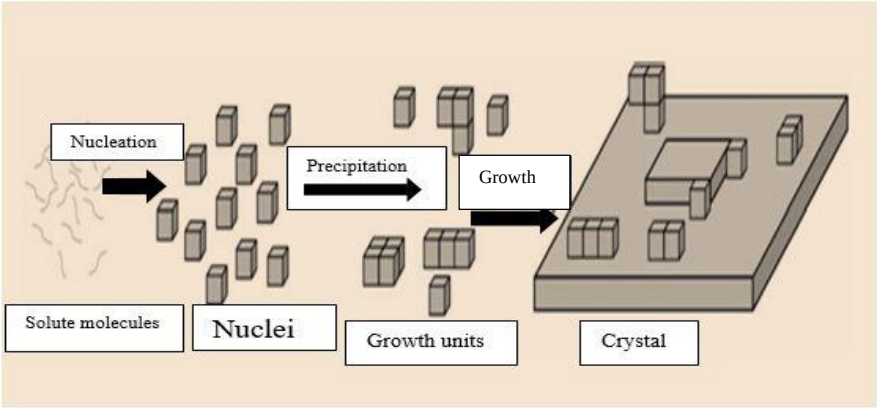

Figure 5: The mechanism of crystal development in a hydrothermal/ solvothermal environment [42].

4.2. Growth Mechanism of Film

A CZTS film was deposited using a solvo/hydrothermal process with the help of a complexing agent. Because it gradually releases metal ions throughout the deposition process, the organic complex agent is critical for producing high-quality thin films. Ostwald's ripening rule is the fundamental principle governing the development of thin films. According to reports, large crystals grow at the cost of smaller crystals [43]. Many tiny crystals form during the start of a system, but almost all of them disappear after a while, except a handful that enlarge. The smaller crystals' nucleation nuclei contribute to the formation of larger crystals. The smaller crystals in the vicinity disappear as the larger crystals expand. During the solution phase reaction, it is common for smaller clusters with a higher number of atoms to form, often resulting in a nucleation process. During the nucleation process, the formation of several smaller particles occurs, resulting in the production of larger particles [43]. CZTS films were formed explicitly due to the progressive liberation of ions from the complexes' dissolution. During a typical reaction bath, metal ions (Cu^{+}, Zn^{2+}, Sn^{4+}) and chalcogen (S^{2+}) constantly move and nucleate on the substrate surface. Following the initial reaction stage, the ions promptly condense under optimal reaction conditions as the reaction time increases. Thus, the formation of the necessary thin layer is identified by observing the step-by-step process of ion-by-ion condensation through the successive accumulation of ions on the surface of the substrate. [45]. Fig. 6 shows the schematic and photograph for film prepared under elevated temperature and pressure.

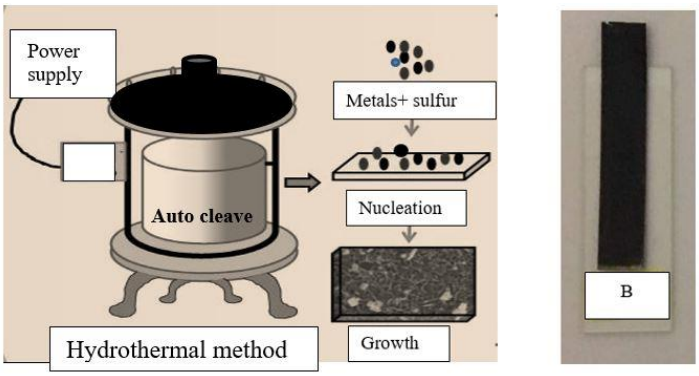

Figure 6: shows the (A) schematic diagram of preparation CZTS film and (B) photograph of CZTS film [46].

5. Effect of Hydro/solvothermal Parameters on Structural, Morphological, and Optical Properties of CZTS

Many papers reported the formation of CZTS NPs/ film using hydrothermal and solvothermal methods [47-48]. Table (2) shows the survey of synthesis of CZTS using hydrothermal and solvothermal methods.

Table 2: The materials source and work conditions of CZTS prepared using solvo/hydrothermal methods.

Material sources	Method	Complex agent	Solvents	Preparation Times (h)	Preparation Temperature (°C)	Ref.
$Cu(CH_3COO)_2$, $Zn(CH_3COO)_2$, $SnCl_2$ and thioacetamide	Hydro-thermal	-	Water	24	200	[47]
$CuCl_2$, $Zn(C_2H_3O_2)_2$, $SnCl_4$ and S	Solvo-thermal	-	Ethylene diamine	16	180	[48]
$CuCl_2$, $Zn(C_2H_3O_2)_2$, $SnCl_4$ and NH_2CSNH_2	Hydro-thermal	-	Water	16	180	[48]
$Cu(CH_3COO)_2$, $Zn(CH_3COO)_2$, $SnCl_2$ and L-cysteine	Solvo-thermal	-	Ethanol	48	400	[49]
$CuCl_2$, $ZnCl_2$, and $SnCl_2$, and NH_2CSNH_2	Hydro-thermal	-	Water	24	200	[50]
$CuCl_2{\cdot}2H_2O$, ($SnCl_2{\cdot}2H_2O$, $ZnCl_2$ and NH_2CSNH_2	Hydro-thermal		Water	20	200	[51]
$CuCl_2$, $ZnCl_2$, and $SnCl_2$ and NH_2CSNH_2	Hydro-thermal	Citric acid	Water	24	190	[52]
$CuCl_2{\cdot}2H_2O$,$ZnCl_2$, $SnCl_4{\cdot}5H_2O$,and NH_2CSNH_2	Solvo-thermal	Polyvinyl pyrrolidone (PVP)	Ethylene glycol	30	180	[53]
$Cu(CH_3COO)_2$,.XH_2O $Zn(CH_3COO)_2$, $SnCl_2$ and NH_2CSNH_2	Solvo-thermal	-	ethylene glycol t	12	180	[54]
$CuCl_2$,$ZnCl_2$, $SnCl_4.5H_2O$,and $SC(NH_2)_2$	Solvo-thermal	-	Ethanol+ Water	24	210	[54]
$CuSO_4$, $Zn(NO_3)_2.6H_2O$, $SnCl_4.5H_2O$, and S	Hydro-thermal	$C_2H_8N_2$	Water	25	200	[56]
Cu $(CH3COO)_2$. H_2O Zn $(CH3COO)_2$. H_2O $SnCL_2$,and $SC(NH_2)_2$	Solvo-thermal	$C_{16}H_{35}N$	Ethenol	4	200	[57]
$ZnCl_2$,$SnCl_2$,$CuCl_2$ and Na_2S	Solvo-thermal	-	Water +HMTM+ $C_2H_8N_2$	18	220	[58]

5.1. Impact of Preparation Temperature

Below is a survey of the last 5 years of studies that show the effect of preparation temperatures on structure, morphology, and optical properties. Pinzón et al. conducted the preparation of Cu_2ZnSnS_4 particles utilising a hydrothermal method, employing various temperature conditions (200 °C, 220 °C, 240 °C, 260 °C, and 280 °C) over 32 hours. Subsequently, the solid materials underwent calcination at 400°C for 2 hours. The structure of CZTS particles was proven to possess a tetragonal geometry. The preferred orientation of the CZTS crystal aligned with the (112) facet. Additionally, all samples exhibited the production of $Cu_{2-X}S$ within CZTS. The transmission electron microscopy (TEM) investigations revealed that, despite undergoing thermal treatment, the sample maintained a nanometric structural shape. The samples demonstrate absorption in the wavelength region of (600–800) nm, indicating a band gap energy of approximately 1.54 eV [59].

Kalyani T. et al. employed an efficient, cost-effective hydrothermal technique to synthesize quaternary CZTS nanostructures. CZTS material characteristics were investigated in detail as a function of reaction temperature (140, 160, 180, and 200) °C. They found pure CZTS obtained at 180˚C and 200 °C. The binary or ternary phase impurities obtained at lower reaction temperatures are due to incomplete reaction. Spherical particles of uniform size that extend from 100 nm to 1 μm were acquired under a temperature condition of 200˚C. The UV-visible

measurement indicated that all samples exhibited strong and broad absorption spectra. The values of the optical band gap estimated from the Tauc plot were (1.10, 1.25, 1.48, and 1.50) eV for samples prepared at (140, 160,180, and 200) °C, respectively [60].

Zheng H. et al. employed the solvothermal method to fabricate CZTS thin films on FTO substrates. The morphology, structure, and optical properties of CZTS thin films were analysed using Scanning electron microscopy (SEM), X-ray diffraction (XRD), Raman spectroscopy, and ultraviolet-visible spectrophotometry. The films were deposited at different temperatures (140 °C, 170 °C, 200 °C, and 230 °C). The XRD and Raman investigations verified the presence of a single phase during the preparation process at temperatures of 230 °C and 200 °C. Nevertheless, the samples synthesized at 140 °C and 170 °C exhibit limited binary and ternary impurities. CZTS thin films at 140°C and 170°C consist of many spherical particles with a typical size range of 300-450 nm. The nano-sized Cu_2ZnSnS_4 thin films produced at 200 °C spread vertically across the FTO substrates. The Cu_2ZnSnS_4 thin films exhibit a composition consisting of spherical particles. When the deposition temperature is raised to 230 °C. However, closer inspection reveals that these particles are composed of many nanorods with dimensions of 200 nm in length and 20 nm in diameter. The samples were found to have high and wide absorbance spectra. The optical band gaps that were retrieved from samples made at 140 °C, 170 °C, 200 °C, and 230 °C are 1.58 eV, 1.54 eV, 1.52 eV, and 1.53 eV, respectively [61].

Satish, S. P. and colleagues successfully synthesized CZTS films using a one-step hydrothermal technique. The researchers investigated the impact of different preparation temperatures (180°C, 200°C, and 220°C) on the structural, morphological, and optical characteristics. The evolution of uniform and densely packed nanospheres and pure kesterite CZTS structure was confirmed by utilizing XRD and field emission scanning electron microscopy techniques. The creation of polycrystalline thin films is confirmed through high-resolution transmission electron microscopy (HR-TEM) and selected area electron diffraction (SAED) analyses. The UV-visible measurements indicated that the films showed intense and broad absorption spectra in the UV-visible region. The optical band gaps were determined to be 1.54 eV, 1.50 eV, and 1.44 eV for samples synthesized at temperatures of 140 °C, 170 °C, 200 °C, and 230 °C, respectively [10]. Table (3) shows the details of solvo/thermal methods based on temperatures. Fig. 7 displays the SEM images of the Cu_2ZnSnS_4 sample prepared at different temperatures. Table (4) shows the effect of preparation temperatures on structure, morphology, and optical band gap for the last twelve years.

Table 3: The details of solvo/hydrothermal methods based on preparation temperatures for the last twelve years.

Metals sources	Sulfur sources	method	Solvents	Preparation Times (h)	Preparation Temperatures (°C)	Ref.
$Cu(NO_3)_2{\cdot}3H_2O$, $Zn(CH_3COO)_2{\cdot}2H_2O$), and ($SnCl_4{\cdot}4H_2O$)	CH_4N_2S	Hydrothermal	Water	24	160, 180, and 200	[62]
Cu, Zn, and Sn powders	S powder	Solvothermal	Absolute alcohol.	18	230, 240, and 250	[63]
$Cu(NO_3)_3 .3H_2O$, $Zn(CH_3COO)_2$, and $SnCl_2$	CH_4N_2S	Hydrothermal	Water	32	200,220,240,260, and 280	[59]
$CuCl_2.H_2O$, $ZnCl_2$, and $SnCl_2.5H_2O$	$C_6H_{12}N_2O_4S_2$	Hydrothermal	Water	30	140, 160, 180, and 200	[60]
$CuCl_2{\cdot}2H_2O$,$ZnCl_2$, and $SnCl_4{\cdot}5H_2O$	C_2H_5NS	Hydrothermal	Water	24	170, 190, 210, and 230	[64]
$CuCl_2{\cdot}2H_2O$,$ZnCl_2$, and $SnCl_2{\cdot}2H_2O$,	CH_4N_2S	Solvothermal	Polyethylene glycol-400 (PEG-400), ethanol (CH_3CH_2OH)	22	160, 170, 180, and 190	[65]
$Cu(CH_3COO)_2.H_2O$, $Zn(CH_3COO)_2.2H_2O$, and $SnCl_2.2H_2O$	CH_4N_2S	Solvotherm	ethylene glycol (EG)	24	180, and 220	[66]
($CuCl_2{\cdot}2H_2O$), $ZnCl_2$, and $SnCl_2{\cdot}2H_2O$	CH_4N_2S	Solvothermal	$H_2C_2O_4$ H_6C_2O	24	140, 170, 200, and 230	[61]
$Cu(CH_3COO)_2{\cdot}2H_2O$, $Zn(CH_3COO)_2{\cdot}2H_2O$, and $SnCl_2$,	CH_4N_2S	Hydrothermal	Water	4	180, 200, 220	[10]

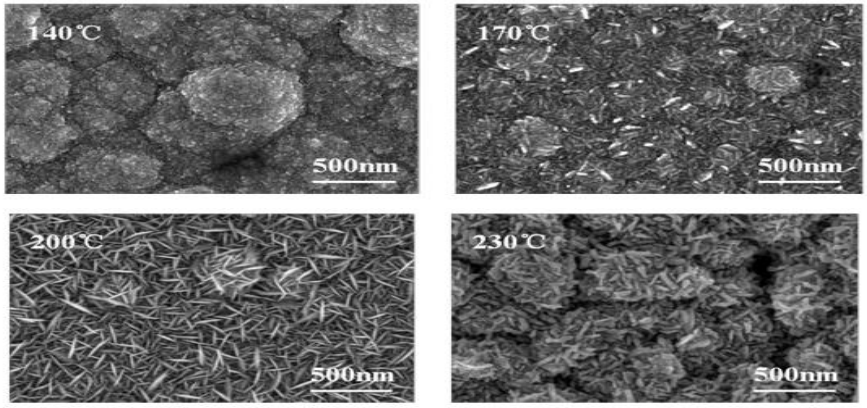

Figure 7: The SEM images of CZTS film prepared at different temperatures [61].

Table 4: The structure, morphology, and optical band gap of CZTS prepared by solvo/hydrothermal method as a function of preparation temperatures for last twelve years.

Preparation temperature °C	Structure	Morphology	Optical band gap eV	Ref.
160	CZTS+$Cu_{2-X}S$	Irregular in shape	1.58	
180	CZTS	Sheet-like structures	1.52	[62]
200	CZTS	Sheet-like structure were cross-connected to form a flower- like	1.50	
230	CZTS+$Cu_{2-X}S$	-	-	[63]
240	CZTS+$Cu_{2-X}S$	-	-	
250	CZTS	Nano-flakes oriented perpendicular to the surface of the substrates	1.45	
170	CZTS+ $Cu_{2-X}S$+ ZnS+ Cu_2SnS_3+ Cu_2SnS_4	Hexagonal nanoplates	-	[64]
190	CZTS+$Cu_{2-X}S$+ Cu_2SnS_4	Hexagonal nanoplates	-	
210	CZTS+ ZnS +Cu_2SnS_3 +Cu_3SnS_4	Agglomeration nanoparticles	-	
230	CZTS	Spherical nanoparticles	1.49	
160	CZTS	Spherical structure	-	[65]
170	CZTS	Agglomeration spherical structure	-	
180	CZTS	Worm-like structure	1.62	
190	CZTS + ZnS	Worm-like structure	-	
180	CZTS	Spherical-like structure	1.45	[66]
220	CZTS	Flower-like structure	1.28	
140	CZTS+ Cu_2SnS_3 +$Cu_{2-X}S$	Spherical structure	1.58	
170	CZTS+ Cu_2SnS_3 +$Cu_{2-X}S$	Spherical structure Nano-sized	1.54	[59]
200	CZTS	Spherical particles composed of a large	1.52	
230	CZTS	number of nanorods	1.53	
140	CZTS+ Cu_3SnS_4, ZnS, and SnS_2 CZTS+ Cu_3SnS_4, ZnS, SnS_2	-	1.10	[60]
160		-	1.25	
180		-	1.48	
200	CZTS	Spherical particles	1.50	
200	CZTS			
200	CZTS+ $Cu_{2-x}S$	Nanometric structure	-	[61]
220	CZTS+ $Cu_{2-x}S$	Nanometric structure	-	
240	CZTS+ $Cu_{2-x}S$	Nanometric structure	-	
260	CZTS+ $Cu_{2-x}S$	Nanometric structure	-	
280	CZTS+ $Cu_{2-x}S$	Nanometric structure	1.50	

180	CZTS	Spherical particles	1.54	
200	CZTS	Spherical particles	1.50	[10]
220	CZTS	Spherical particles	1.44	

This survey shows that as preparation temperatures increase, the crystal structure improves, and the secondary phases disappear.

Elevated temperatures can enhance the creation of a desired crystal structure by aiding a restructuring of atoms and permitting the movement of particles to obtain the desired crystal arrangement. Furthermore, the preparation temperature plays a vital role in the development of the secondary phase in CZTS. Cu_2ZnSnS_4 can undergo the formation of secondary phases as a result of impurities, defects, or non-stoichiometric compositions. The secondary phases may exhibit distinct crystal structures and chemical compositions in contrast to the desired CZTS phase, such as the presence of copper sulphide (Cu_2S) or zinc sulphide (ZnS) phases. At high temperatures, the stability of the desired CZTS phase can be favored over the secondary phases. The increased energy and mobility of atoms at high temperatures allow for the rearrangement of atoms, leading to the dissolution or transformation of secondary phases into the desired CZTS phase (single phase) [59, 63].

The investigation also reveals that the morphology and form of CZTS grains alter with different processing temperatures. Grain growth is accelerated at high temperatures because atomic and ionic motion is enhanced. This has the potential to make the film surface smoother and the grain sizes larger. Submicron grains and coarser surfaces could be the outcome of reduced atomic mobility caused by lower temperatures. Under specific temperature conditions, certain crystallographic planes or directions may experience accelerated growth rates, resulting in a preference for growth in particular directions. This leads to the formation of elongated or faceted grains [61, 62].Finally, the survey shows the effect of preparation temperatures on energy gap values. Due to the preparation, temperature can affect the composition of CZTS. CZTS can contain various defects, such as vacancies, anti-site defects, and interstitials. The preparation temperature can influence the formation and concentration of these defects. Defects can introduce energy levels within the band gap, affecting the energy gap of CZTS. Higher temperatures generally promote better crystallization and larger grain sizes. The presence of grain boundaries and crystal defects can influence a material's electrical characteristics, specifically affecting the energy gap. [64-66].

5.2. Impact of Preparation Times

The following is a review of the last five years of research on the effect of times of preparation on structural, morphological, and optical properties.

Satish S. P. et al. effectively achieved the synthesis of affordable CZTS nanocrystalline thin films at different reaction durations (3, 4, 5, and 6) h using a single-step hydrothermal method. The structural, morphological, and electrochemical features of the CZTS films were examined to explore the impact of hydrothermal reaction duration on their growth. Structure properties revealed the formation of pure nanocrystalline keserite CZTS films. In addition, the structure analysis showed that the crystallinity of films improved as reaction time increased. SEM images showed that the CZTS particles looked like nanograins. The optical investigations revealed that the Cu_2ZnSnS_4 films had high absorbance spectra with a decrease in optical band gap energy from 1.52 eV to 1.41 eV [11]. In a study by Kasim I. M. et al., CZTS particles were produced using the hydrothermal technique and subsequently applied onto a substrate using the doctor-blading technique. Inspection of the structure revealed the presence of Kesterite CZTS NPs. Analysis of samples prepared for (12, 36, and 48) h showed that secondary phases were present, specifically SnS and $Cu_{2-X}S$, inside the CZTS compound. However, the sample prepared for 24 hours exhibited the creation of a single-phase CZTS compound. After 12 hours, the hydrothermal reaction resulted in the prevalence of uniformly distributed spherical flower-like particles in the sample. Spherical particles with a homogeneous composition were observed after 24 hours of reaction time. Particles resembling flowers began to agglomerate together after 36 h. The particles underwent additional aggregation, forming larger agglomerates after 48 hours of reaction time. UV-visible spectra showed high absorption spectra with energy gap values equal to 1.52 eV, 1.51eV, 1.51eV, and 1.52 eV for samples prepared for 12 h, 24 h, 36 h, and 48 h, respectively [67]. Table (5) shows the details of the solvo/hydrothermal method based on time. Fig. 8 shows the

SEM images for CZTS film prepared at various times. Table (6) shows the structure, morphology, and optical band gap of CZTS prepared by solvo/hydrothermal method as a function of preparation time.

Table 5: The details of solvo/thermal methods based on times.

Metals sources	Sulfur sources	Method	Solvents	Preparation Times (h)	Preparation Temperatures (°C)	Ref.
$CuCl_2 \cdot 2H_2O$,$ZnCl_2$, and $SnCl_4 \cdot 5H_2O$,	CH_4N_2S	Hydrothermal	Water	0.5, 1,3, 6,12,and 24	190	[68]
$CuCl_2 \cdot 2H_2O$, $ZnCl_2$, and $SnCl_2$	CH_4N_2S	Hydrothermal	Water	3,4,5, and 6	180	[11]
$CuCl_2.2H_2O$, $ZnCl_2$, and $SnCl_4.5H_2O$	C_2H_5NS	Hydrothermal	Water	12, 24, 36, and 48	150	[67]
CuCl, $ZnCl_2$, and $SnCl_4.5H_2O$	CH_4N_2S	Hydrothermal	Water	18, 24, and 30	200	[69]

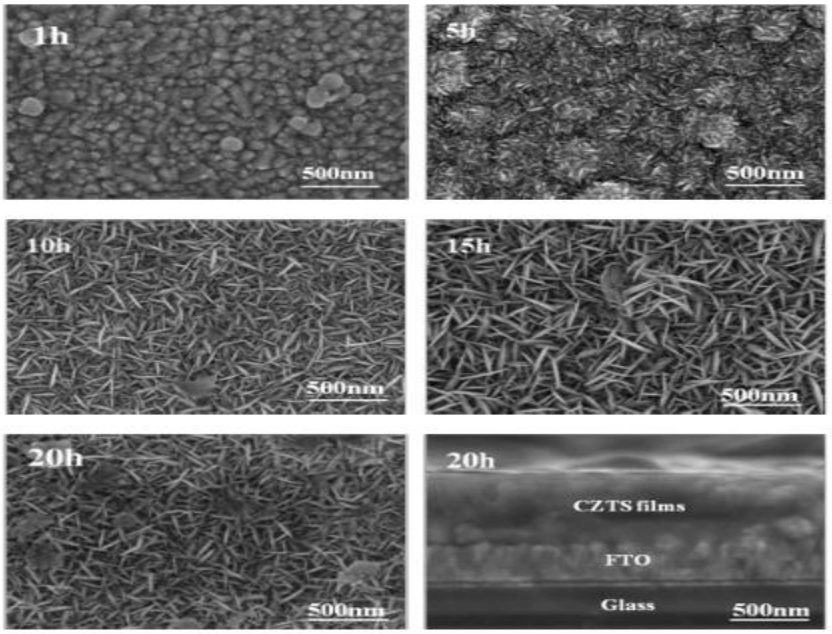

Figure 8: The SEM images of CZTS film prepared at different times [61].

Table 6: The structure, morphology, and optical band gap of CZTS prepared by solvo/hydrothermal method as a function of preparation time for last twelve years.

Preparation time h	Structure	Morphology	Optical band gap eV	Ref.
18	CZTS+ZnS	Agglomeration and a shape resembling plates	-	[11]
24	CZTS+ZnS	Agglomeration and a shape resembling plates	-	
30	CZTS	Agglomeration and a shape resembling plates	1.70	
3	CZTS+ CuS	Microsphers	-	[67]
6	CZTS+CuS	Microsphers	-	
12	CZTS	Nanosheet	-	
24	CZTS	Nanosheet	1.45	
12	CZTS+ SnS+ $Cu_{2-X}S$	Spherical flower-like particles	1.52	[68]
24	CZTS	Spherical flower- like particles	1.51	
36	CZTS+ SnS+ $Cu_{2-X}S$	Agglomeration of flower-like particles	1.51	
48	CZTS+ SnS+ $Cu_{2-X}S$	Larger Agglomeration of flower-like particles	1.52	
3	CZTS	Nanograin	1.52	[69]
4	CZTS	Nanograin	1.48	
5	CZTS	Nanograin	1.46	
6	CZTS	Nanograin	1.41	

This review shows that as preparation time changes, the structure, morphology, and band gap change. This is due to. During the preparation process, the structure of a material can evolve and transform over time. Increasing the preparation time allows for more extensive atomic rearrangements, forming a more thermodynamically stable crystal structure [67, 69]. In addition, more atoms or molecules can nucleate and grow during longer preparation times, resulting in more extensive and well-developed structures. This phenomenon can result in bigger grains, enhanced uniformity in film thickness, and increased surface smoothness. In addition, extended preparation durations can facilitate the merging of smaller particles, leading to alterations in the overall structure and distribution of particle sizes [11, 69]. Finally, extended preparation periods can enhance crystallinity and reduce structural flaws, leading to a more precise electrical band structure. These effects can alter the material's electrical transitions and energy levels, resulting in modifications to the optical band gap. Furthermore, longer preparation durations can facilitate the elimination of contaminants or undesired chemical components, which can impact the energy levels and band structure, thereby altering the material's optical characteristics [68].

5.3. Impact of Complex Agent Types and Concentrations

The five years of research that demonstrate how complex agent types and concentrations affect structural, morphological, and optical properties are summarised here.

Cristóbal J. D. et al. successfully fabricated Nanoparticles (NPs) of Cu_2ZnSnS_4 by microwave hydrothermal route for different Polyvinyl pyrrolidone (PVP) surfactant weights. XRD and Raman's measurements examined kesterite CZTS NP production. These tests also showed single-phase CZTS nanoparticles in PVP samples. The sample without PVP creates secondary $Cu_{2-X}S$ phases in CZTS nanoparticles. TEM and STEM were used to observe the synthesized material without PVP. Nanoparticle agglomerates with an average size of 1650 nm were found. The NP agglomeration size was 210 nm, 560 nm, 550 nm, 450 nm, and 350 nm for 0.04 g, 0.16 g, 0.32 g, 0.64 g, and 0.128 g of PVP content, respectively. The results show that increased PVP concentrations lead to larger agglomerates. The optical properties showed high absorbance spectra, and the sample prepared using 0.64 g of PVP showed the highest absorbance spectra compared with the other samples. The energy gap values were 1.73 eV, 1.56 eV, 1.77eV, 1.58 eV, 1.76 eV, and 1.72 eV for samples prepared using 0 g, 0.04 g, 0.16 g, 0.32 g, and 0.64 g respectively [70].

Yas A. and colleagues successfully synthesized pure kesterite CZTS nanocrystals using solvothermal. XRD and Raman spectroscopy revealed single-phase CZTS nanoparticles in the 2 mg/mL glycine sample. Other samples showed secondary phase development. The 0.5 and 1 mg/mL films had rough granular structures with obvious holes. The surface shape improved when the glycine complex agent was 1.5 mg/mL and grain size was (1-1.4) µ. A 2 mg/mL glycine concentration resulted in a smooth, compact, crack-free thin film with grains ranging from 2 to 2.8 µ. The strong absorbance spectra were seen in the 300-1000 nm range of the optical spectra of the Cu_2ZnSnS_4 nanocrystals. The glycine concentration affected the Eg values: 0.5 mg/ mL, 2.27 eV; 1 mg/mL, 1.77 eV; 1.5 mg/mL, 1.64 eV; and 2.0 mg/mL, 1.54 eV [71].

Feng L. et al. used a solvothermal method to develop CZTS particles using diethylenetriamine (DETA). XRD and Raman investigations showed that DETA-treated samples generated pure CZTS nanoparticles (1:4, 1:2), while DETA-free samples formed CuS. CZTS surface structure was examined by SEM. Different nanoparticle forms were evident in the samples. Increases in DETA concentration resulted in less nanoparticle aggregation. In optical investigation, DETA-prepared samples with DETA volume to total volume ratios of 0:1, 1:4, and 1:2 have energy gaps of 1.85, 1.59, and 1.53 eV [72]. Table (7) shows the details of solvo/thermal methods based on complex agents. Fig. 9 shows the TEM images for CZTS film prepared using different complex types [72]. Table (8) shows the structure, morphology and optical band gap of CZTS prepared by solvo/hydrothermal method as a function of complex agent types and concentration.

Table 7: The details of solvo/thermal methods based on complex agent.

Metals sources	Sulfur sources	Complex agents	Solvents	Times (h)	Temperature (°C)	Ref.
$CuCl_2.2H_2O$, $ZnCl_2$, and $SnCl_2.2H_2O$	CH_4N_2S	CTAB (0 M, 0.002 M, 0.004 M, and 0.00625 M)	$H_2C_2O_4$	24	200	[72]
$Zn(NO_3)_2{\cdot}6H_2O$, $CuSO_4$ and, $SnCl_2{\cdot}2H_2O$	CH_4N_2S	PVP(0, 1.28, 0.64, 0.32, 0.16 and 0.04 g)	ethylene glycol	0.2	200	[74]
$CuCl_2{\cdot}2H_2O$, $ZnCl_2$, and $SnCl_2{\cdot}2H_2O$	CH_4N_2S	glycine solutions (0.5,1,1.5, and 2 mg/mL)	Oleylamine	14	240	[75]
$CuCl_2{\cdot}2H_2O$, $ZnCl_2$, and $SnCl_2 \cdot 2H_2O$	S	DETA	Water+ ethanol absolute	12	180	[73]
$Cu(CH_3COO)_2$, $Zn(CH_3CO_2)_2{\cdot}2H_2O$, and $SnCl_2$	thioacetamide	hydrazine, Na_3-citrate, and Na_2EDTA	Water	24	200	[74]

Table 8: The relationship between complex agents and the structure, morphology, and optical band gap.

Complex agent Concentration and type	Structure	Morphology	Optical band gap eV	Ref.
Without complex	CZTS	-	1.67	[72]
Hydrazine	CZTS	-	1.51	
Na_3-citrate	CZTS	-	1.44	
Na_2-EDTA	CZTS	-	1.5	
0 M CTAB	CZTS+ Cu_3SnS_4	Non-uniform and loosely aggregated structures	1.5	[73]
0.002 M CTAB	CZTS+ Cu_3SnS_4	Flower- like microsphere compos of small nano-sheet	1.40	
0.004 M CTAB	CZTS+ Cu_3SnS_4	Flower- like microsphere compose small nano- sheet	1.5۲	
0.00625 M CTSB	CZTS+ Cu_3SnS_4	Flower- like microsphere compose of small nano-sheet	1.54	
0 PVP	CZTS +$Cu_{2-x}S$	Nanoparticle agglomerates	1.73	[74]
0.04 g PVP	CZTS	Spherical-shaped agglomerates	1.56	
0.16 g PVP	CZTS	Spherical-shaped agglomerates	1.77	
0.32 g PVP	CZTS	Spherical-shaped agglomerates	1.58	
0.64 g PVP	CZTS	Spherical-shaped agglomerates	1.76	
0.128 g PVP	CZTS	Spherical-shaped agglomerates	1.72	
0 DETA			1.85	[70]
1:4 (volum to total volum) DETA	CZTS+ CuS	Different shape of nano-particles	1.59	
	CZTS	Different shape of nano-particles		
1:2 (volum to total volum) DETA	CZTS	Different shape of nano-particles	1.53	
0.5 mg/mL glycine complexing agent	CZTS+ $Cu_{2-x}S$	Rough granular structure + visible pores	2.27	[71]
1 mg/mL glycine complexing agent	CZTS+ $Cu_{2-x}S$	Rough granular structure + visible pores	1.77	
1.5 mg/mL glycine complexing agent	CZTS + $Cu_{2-x}S$	Better rough granular structure	1.64	
2 mg/mL glycine complexing agent	CZTS	Better rough granular structure	1.54	

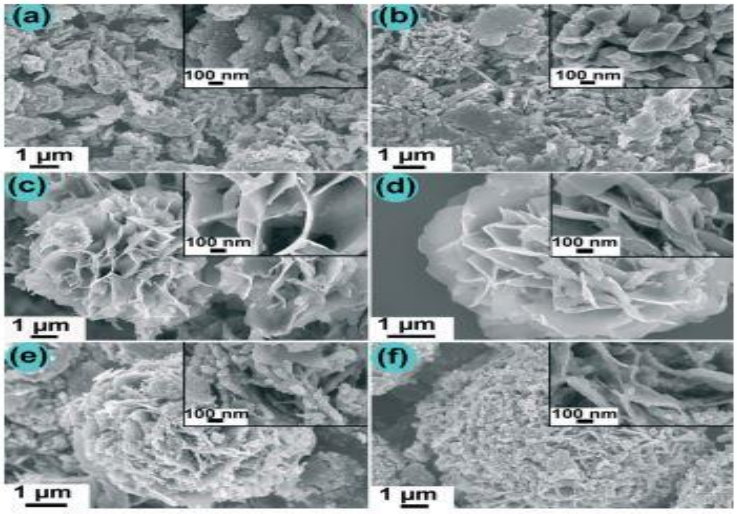

Figure 9: The FESEM images of CZTS film prepared with different of citric acid at 190 °C for 24 h. (a) 0 mmol (b) 1 mmol (c) 2 mmol (d) 4 mmol (e) 8 mmol (f) 16 mmol [68].

The notice from this review is the influence of types and concentrations of complex agents on the structure, morphology, and optical band gap of CZTS. These agents can interact with metal ions, control their coordination environment, and influence the crystal growth and nucleation processes. By selecting appropriate complex agents. It is feasible to facilitate the development of the intended kesterite phase while inhibiting the production of undesired secondary phases. As well, Complex agents can also influence the morphology of CZTS materials. They can act as shape-directing agents, controlling crystal facets' growth rate and direction. They can also prevent particle agglomeration, influencing the overall morphology, size, and distribution of CZTS particles or thin film features. Finally, complex agents can influence the formation of defects, impurities, or surface states within the material. These defects can introduce additional energy levels within the band gap, affecting the absorption and emission properties. [70, 72, 73].

5.4. Impact of Thiourea Concentrations and Sulfur Sources

This text presents a review of recent studies that examine the influence of thiourea concentration and sulphur sources on the structural, morphological, and optical features. These studies were published within the last five years. Mkawia E. et al. M. successfully developed CZTS NPs by the solvothermal route. They studied the influence of the sulfur sources (Thiourea, atrium thiosulfate, L-cystine, and methionine) on the properties of CZTS NPs. XRD and Raman analyses exhibited the preparation of pure Cu_2ZnSnS_4 NPs. Also, the SEM images revealed that the nanoparticles synthesized using thiourea for 12 hours exhibited consistent and clearly defined spherical particles, with sizes ranging from 50 to 80 nanometers. The energy gap value of the Cu_2ZnSnS_4 NPs formed using thiourea equalled 1.51 eV. Table (9) shows the details of solvo/thermal methods based on thiourea concentrations and sulfur source. Table (10) shows the structure, morphology, and optical band gap of CZTS prepared by solvo/hydrothermal method as a function of thiourea concentrations and sulfure source. Fig. 10 shows the SEM images for CZTS film prepared as a function of thiourea concentrations and sulfur source [75].

Table 9: The details of solvo/thermal methods based on thiourea concentrations and sulfur sources.

Metals sources	Sulfur sources	Method	Solvents	Times (h)	Temperature (°C)	Ref.
$CuCl_2.2H_2O$, $ZnCl_2$, and $SnCl_2.2H_2O$	CH_4N_2S (0.15 M, 0.2 M, 0.25 M and 0.325 M)	Solvothermal	$H_2C_2O_4$	24	200	[74]
$CuCl_2$, $ZnCl_2$, and $SnCl_2{\cdot}2H_2O$	CH_4N_2S (10,15,20,25 and,30) mmole	Hydrothermal	$C_4H_{13}N_3$	72	180	[75]
$CuCl_2.2H_2O$, $ZnCl_2$, and $SnCl_4.5H_2O$	CH_4N_2S, C_2H_5NS, and Na_2S	Hydrothermal	Water	24	240	[76]

$CuSO_4 \cdot 5H_2O$, $ZnCl_2 \cdot 2H_2O$, and $SnCl_2$	$(CS(NH_2)_2$,$Na_2S_2O_3$, $C_6H_{12}N_2O_4S_2$,and $C_5H_{11}NO_2S$	Solvothermal	Ethylene glycol.	14	240	[77]

Table 10: The structure, morphology and optical band gap of CZTS prepared by solvo/hydrothermal method as a function of thiourea concentrations and sulfur sources types for twelve years.

Thiourea concentrations and sulphur source	Structure	Morphology	Optical band gap eV	Ref.
Na_2S	CZTS	Nano particlres	-	
C_2H_5NS	CZTS	Nano particles	1.51	[75]
CH_4N_2S	CZTS+ Cu_7S_4 + Cu_2SnS_3	Nano particles	-	
0.15 M Thiourea	CZTS	Uniformly shaped spherical particles	1.37	
0.2 M Thiourea	CZTS	Uniformly shaped spherical particles	1.41	[76]
0.25 M Thiourea	CZTS	Microsphers look like flower	1.52	
0.32 M Thiourea	CZTS	Nano sheet look like flower	1.54	
10 m mole thiourea	CZTS+ ZnS+ SnS+SnS_2+ $Cu_{2-X}S$	Flakes	-	
15 m mole thiourea	CZTS+ZnS+SnS+SnS_2+ $Cu_{2-X}S$	Flakes	-	
20 m mole thiourea	CZTS+ZnS+SnS+SnS_2+ $Cu_{2-X}S$	Flakes	-	[77]
25 m mole thiourea	CZTS	Flakes	-	
30 m mole thiourea	CZTS	Flakes	1.45	
Thiourea	CZTS	Sphere- like particles	1.51	
Atrium thiosulfate	CZTS	-	-	[74]
L- cysteine	CZTS	-	-	
Methionine	CZTS	-	-	

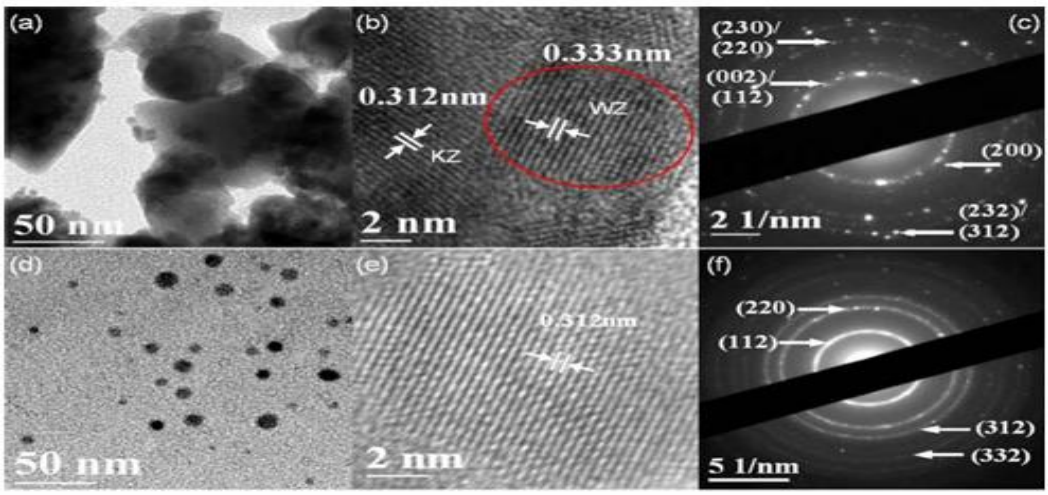

Figure 10: TEM, HRTEM images and SAED patterns of CZTS_TAA (a, b, c) and CZTS_Na_2S (d, e, f) nanoparticle [77].

As shown in the study, the influence of sulfur concentrations on structural, morphological, and optical band gaps is due to the sulfate source providing the sulfur required to form CZTS. The availability of sulfur ions during the reaction or deposition process can impact the formation of CZTS and crystal structure. Sulfate sources with higher sulfur availability promote the formation of stoichiometric CZTS with the desired crystal structure. The sulfate source can affect the reaction kinetics and sulfur incorporation into the CZTS structure. Different sulfate sources can have different reactivity or dissolution rates, influencing the reaction speed and availability of sulfur ions during synthesis. The choice of sulfate source and concentrations can influence the formation of sulfur defects in CZTS materials. Sulfur vacancies or interstitial sulfur atoms can act as defect states within the CZTS band gap, affecting its electronic and optical properties [74-77].

5.5. Impact of other parameters

Mahesh S. et al. successfully prepared CZTS NPs using a one-step hydrothermal route. They studied the influence of pH values (4.3, 5, 7, and 9) on structural, morphologic, and optical properties. According to XRD and Raman measurements, the pH 7 samples formed single-phase kesterite CZTS nanocrystals. At pH=4.3 and pH=5, $CuSnS_3$, $Cu_{2-X}S$, and SnS_2 formed, whereas at pH=9, they formed too. The BF-TEM images of CZTS NCs at pH=7 showed uneven, polydispersed crystals. The optical band gap energy of synthesized nanoparticles was 1.5, 1.2, 1.44, and 1.28 for samples prepared at 4.3, 5, 7, and 9, respectively [74]. This is due to the higher concentration of OH ions compared to H ions, which enhances the hydrolysis of thiourea. As a result, sulfur ions are released, leading to the formation of CZTS. The changes in surface morphology resulting from a change in pH values are attributed to the modification in the equilibrium constant of the reaction and condensation processes, thus affecting the surface morphology. Finally, pH variations can alter the concentration of impurities, defects, or sulfur vacancies within the CZTS structure, which can modify the electronic band structure and optical transitions. Different pH conditions can lead to variations in the band gap energy, absorption coefficient, and optical band edge of CZTS materials, influencing their photovoltaic or optoelectronic characteristics [78].

Vanalakar S.A. et al. fabricated CZTS NPs using the hydrothermal method. The XRD and Raman investigations revealed the presence of ZnS, Sn_2S_3, and SnS compounds within the CZTS NPs in the sample generated using deionized water DW. The sample was prepared using ethylene diamine EN and DW solvents, incorporating ZnS inside the CZTS material. Additionally, the sample generated using the combination of Sodium dodecyl sulfate SDS and DW consists of Sn_2S_3 and ZnS within CZTS. The change in structure is due to the solvent type, which can impact the solubility of precursor compounds and the dissolution of reactants. Different solvents have varying abilities to dissolve metal salts or organometallic precursors used in CZTS synthesis. Solvents with higher solubility for the precursor compounds can facilitate their dissolution, leading to better homogeneity and reactivity during subsequent reactions. The choice of solvent can influence the availability of metal ions and sulfur species, affecting the formation of CZTS and its crystal structure. The CZTS: DW sample has particles 20 nm and is more significant in a non-uniform distribution. DW+EN produced nanoparticles with a diameter of 10 nm or more. SDS+DW samples had 4–8 nm particles. This may be due to the choice of solvent, which can result in different fluidic properties and surface interactions, leading to particle shape, size, and aggregation behavior variations. Solvents with specific surface energies or surface-active properties can influence surface diffusion and attachment kinetics, forming specific morphologies. The band gap energy values for the CZTS: DW, CZTS: WD +EN, and CZTS: WD+SDS samples were determined to be 1.53 eV, 1.55 eV, and 1.85 eV, respectively [76]. The change in band gap values as the change in solvent types may be related to solvents, which can influence the electronic structure of CZTS by altering the surface states or surface electronic properties. The presence of solvents can modify the distribution of charge carriers, introduce surface traps, or modify the band alignment at the CZTS surface. The alterations in the electronics structure can impact the band gap, energy levels, and optical characteristics of CZTS [79].

Yahong X. et al. successfully prepared hierarchical CZTS nanostructures using a solvothermal approach. They studied the effect of zinc concentrations (0.005 M, 0.02 M, and 0.05 M) on structural, morphological, and optical properties. The XRD analysis confirmed the formation of single-phase CZTS NPs in all samples. A Cu_2ZnSnS_4 hierarchical nanostructure, like a flower, was successfully synthesized at a zinc concentration of 0.005 M. The average diameter of the nanostructure was around 2 mm. At 0.02 M zinc concentration, a structure with a mixture of hierarchical rods, hierarchical spheres, and particles was observed. Nanoparticles with average sizes ranging from 50 nm to 60 nm were produced under conditions with a zinc concentration of 0.05 M, exhibiting a virtually uniform and monodisperse distribution. CZTS properties change as Zinc concentration changes due to Zn atoms acting as nucleation centers. Table 11. Shows the details of solvo/thermal methods based on temperatures. Fig. 11 shows the SEM images for CZTS film prepared with various zinc concentrations [80].

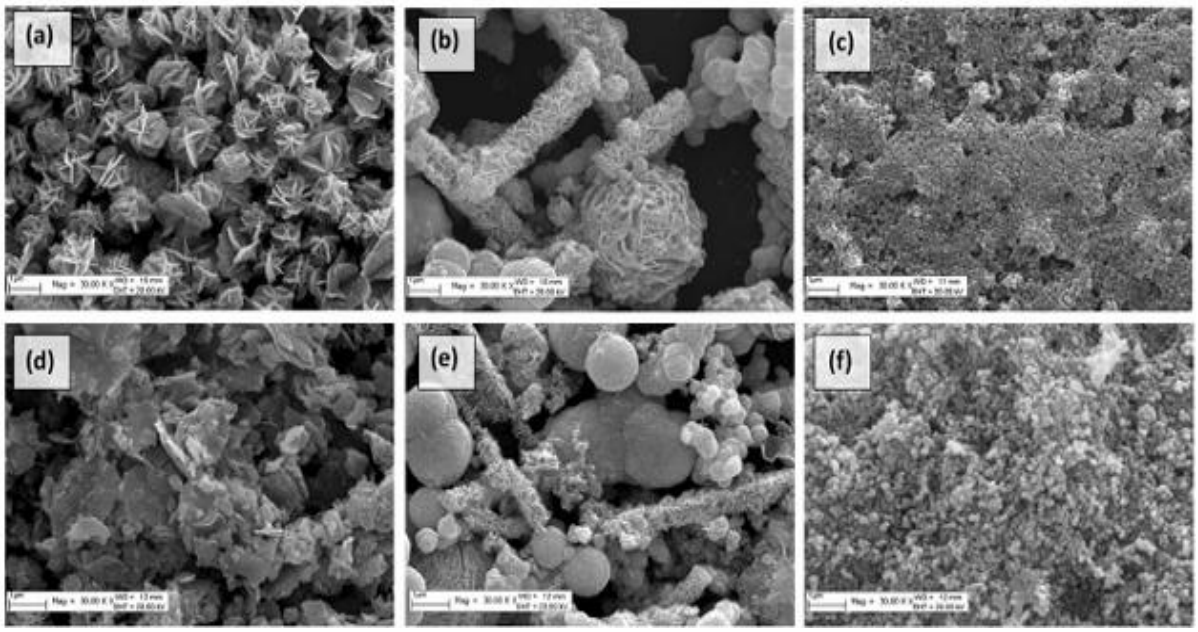

Figure 11: SEM images of CZTS prepared with various zinc concentrations before annealing (a) 0.005 M, (b)0.02 M, and (c) 0.05 M. and SEM images of CZTS prepared with various zinc concentrations after annealing (d) 0.005 M, (e)0.02 M, and (f) 0.05 M [80].

Table 11: The details of solvo/thermal methods based on other parameters.

Metals sources	Sulfur sources	Parameters	Solvents	Time (h)	Temperature (°C)	Ref.
$Cu(CO_2CH_3)_2$, $Zn(CH_3CO_2)_2$, and $SnCl_2$	Thioacetamide	Various pH values (4.3, 5,7, and 9)	Water	24	200	[78]
$ZnCl_2$, $CuCl_2$, and $SnCl_2$	Na_2S	Various types of solvents	DW,DW+EN,and DW+SDS	18	180	[79]
$CuCl_2.2H_2O$, $ZnCl_2$, and $SnCl_4.2H_2O$,	Thiourea	Various zinc concentration(0.005, 0.02, and 0.05) M	Water	48	200	[80]

The influence of hydro/solvothermal parameters on the structure, morphology, and optical properties of CZTS has been studied, and the following results have been discovered: The significant impact of preparation temperature on structure, morphology, and optical band gap. Also, the optimum preparation temperature is 200 °C. Preparation time, complex agent, and thiourea have an excellent impact on structure and energy gap while showing that they play a less influential role on morphology. The optimum preparation time is 24 h, and the optimum pH is 9. Different shapes are formed by using the solvo/hydrothermal method. Finally, there is a lack of studies on the effect of Sn, doping CZTS, and co-doping CZTS prepared by solvo/hydrothermal method.

6. Overview of Literature

Various techniques can be employed to fabricate CZTS on diverse substrates. Such as sputtering, thermal evaporation, laser ablation, pulsed laser deposition, sol-gel, spray pyrolysis, chemical vapor deposition, spin coating electrodeposition, and SILAR [47-53]. The hydro/solvothermal method has been widely utilized as a chemical method to synthesize high-quality nanocrystals with distinctive morphology, crystal structure, and low-cost manufacturing [52-57]. Numerous studies have been done on the solvothermal and hydrothermal processes for forming CZTS film and powder for photovoltaic applications. In 2013, Sekou et al. developed CZTS-based photoelectrochemical cells using hydrothermal with assistance spin coating [81]. Aixiang et al. effectively produced a heterojunction solar cell in 2014 by employing a solvothermal process with CTAB as a complicated

agent [70]. 2015, Yaohan et al. used the solvothermal approach to prepare a CZTS-based photoelectrochemical cell [61]. In 2018, Shih-Jen Lin fabricated a CZTS-based perovskite solar cell using the hydrothermal method with spin coating assistance [82]. In 2021, Satish et al. successfully synthesized CZTS-based photoelectrochemical cells using the hydrothermal method [10]. Table (12) shows the literature Survey on using the solvo/hydrothermal method for preparing CZTS compound for photovoltaic application.

Table 12: The literature survey of using the hydro/solvothermal method for preparing CZTS compound for photovoltaic application.

Preparation method	Solar cell structure	V_{OC} (mV)	I_{SC}	η%	Application	Ref.
Solvothermal+ spin coating methods	FTO/TiO_2/$CH_3NH_3PbI_3$/CZTS/Au	821	13.20 mA/cm^2	6.24 ± 0.35	Perovskite solar cell	[71]
Solvothermal Method	FTO/CZTS/electrolyte/graphite interfacial	733	5.56 mA/cm^2	1.18	Photoelectrochemical (PEC) cell	[61]
Hydrothermal + doctor blading	Counter electrodes: CZTS/TiO_2/FTO Photoelectrodes : Tio_2/$TiCl_4$/FTO	763	13.253 mA/cm^2	6.24	Dye-sensitized solar cell	[83]
One-pot hydrothermal roue	FTO/CZTS/$Eu(NO_3)_3$/graphite	771	3.28 A/cm^2	4.87	Photoelectrochemical (PEC) cell	[10]
Hydrothermal + doctor blading	Counter electrodes: CZTS/FTO Photoelectrodes : Tio_2/TiO_2/FTO	460	9.2 mA/cm^2	2.65	Dye-sensitized solar cell	[84]
Hydrothermal + doctor blading	FTO/CZTS/Na_2SO_4/Pt	580	8.87 mA/cm^2	2.98	Photoelectrochemical (PEC) cell	[85]
Hydrothermal+ spin coating	ITO/(CZTSNP$_S$+PEDOT:PSS)/ $MAPbI_3$/C60/BCP/Al	840	19 mA/cm^2	7.55	Perovskite solar cell	[86]
Solvothermal+ spin coating methods	Counter electrodes: CZTS-MWCNTs Photoelectrodes: DS-TiO2/FTO	760	16.6 mA/cm^2	9.04	Dye-sensitized solar cell	[87]
Solvothermal method	FTO/CZTS/CdS/i-ZnO/ZnO:Al	220	1.40 mA/cm^2	0.162	Heterojunction solar cell	[88]
Solvothermal method	Counter electrodes: CZTS/FTO Photoelectrodes : N719/$TiCl_4$/TiO_2/FTO	730	13.4 mA/cm^2	6.13 ±0.21	Dye-sensitized solar cell	[89]

7. Challenges and Solutions to Enhance the Performance of Solar Cells Based on CZTS

The survey table indicates that the manufacture of CZTS-based solar cells using the solvo/hydrothermal approach is currently being researched, and there is a continuing attempt to enhance their efficiency. Despite significant progress in achieving higher photovoltaic (PV) efficiencies for CZTS thin solar cells, the reported efficiencies of the best device still fall short of the theoretically estimated efficiency of approximately 31%.The efficiency of CZTS-based solar cells remains relatively low in comparison to previously reported efficiencies due to kesterite experts widely agree that the V_{OC} (voltage open circuit) is the primary limiting factor for kesterite-based thin film solar cells (TFSCs). However, the exact cause of this limitation is still a subject of ongoing disagreement among researchers. To increase the V_{OC}, the concentration of Cu_{Zn} antisite defects caused by Cu and Zn intermixing must be reduced, which can be accomplished by substituting other large-size elements/atoms for Zn or Cu, which may prevent the formation of defects and thus improve sample quality. So, developing alternative novel materials is essential in improving the performance of CZTS solar cells [90]. In addition to the V_{OC} deficit, non-uniformity of the film's considerable series resistance, low fill factor, low shunt resistance, faster electron-hole recombination at the junction, non-post-annealing in sulfur or selenide environment involved in the manufacture of CZTS solar cells results in poor quality film thus enhancing recombination thereby resulting in poor solar cell device performance.

Also,Cliff-like band alignment, interfacial flaws, and inadequate band bending are critical issues in heterojunction optimization. Alternative buffer layers with enhanced CBM are especially desirable for CZTS with a wide bandgap. The $Zn_{1-x}Cd_xS$ buffer generated from the CdS buffer affords favorable spike-like band alignment and spontaneous interface passivation. With this buffer, efficiency is above 10%, and additional optimization is conceivable because recombination is still interface-dominated. On the other hand, Cd-free buffers are more environmentally benign and may lower the blue light parasitic absorption and lattice mismatch associated with the CdS buffer. Because of the passivation effects of the self-formed Zn(S, O) phase during deposition, the ALD-ZTO buffer layer is a better choice. Passivation layers could also be added to enhance the quality of the interface [91]. Some dielectric materials with suitable characteristics could provide field and chemical passivation, preventing interfacial recombination. The device performance is negatively affected by the over-chalcogenization of Mo and the decomposition of kesterite at the back interface between them. Implementing an intermediary layer at the kesterite/Mo interface is viable. To successfully suppress the expansion of molybdenum chalcogenide, 1- a quantity of less than 5 nm of CAO and CuO is sufficient. 2-Furthermore, certain p-type materials with high-work function, referred to as HTL, provide advantageous carrier selectivity and passivation effects. 3-Thus, more HTL materials can be investigated to meet kesterite's specific back contact needs. 4-The self-organized nanopattern Al_2O_3 layer may be a more favorable intermediate material due to the advantages of maintaining local contact between kesterite and Mo [92]. One potential method for improving the performance of photovoltaic (PV) devices is to explore alternate device topologies, such as tandem structures. An alternative method proposed to enhance the device's efficiency involves annealing in an atmosphere containing sulfur or selenium to acquire superior-quality crystals. Overall, as our comprehension of the loss mechanism in kesterite solar cells becomes more profound, numerous feasible strategies have been identified. While consistently investigating novel optimizations, it is crucial to take a comprehensive approach to incorporate these tactics grounded in many mechanisms.

8. Conclusions

Nowadays, Kesterite CZTS has attracted the interest of researchers because of its fascinating features. Many chemical synthesis routes, including sol-gel, spray pyrolysis, hydrothermal, and solvothermal have revealed some benefits and disadvantages for the preparation of CZTS. Hydrothermal and solvothermal are simple, non-toxic, inexpensive processes. The structure, morphology, and optical properties of CZTS depend heavily on hydrothermal and solvothermal parameters such as preparation temperature, preparation time, complex agent type, and source of sulphur. The preparation temperature plays a great role in the structure, morphology, and optical energy gap. In addition, preparation time shows a small impact on morphology. All parameters show a good impact on structure and optical band gap. The challenges faced by CZTS-based solar cells were discussed and we found a suitable solution. We suggest these works as future works: 1- study the effect of Sn concentrations on CZTS prepared by hydrothermal and solvothermal methods, prepared doping-CZTS and co-doping CZTS by solvo/hydrothermal method, fabricated doping, and co-doping CZTS based dye sensing solar cell, and perovskite solar cell, fabrication doping-CZTS based heterojunction solar cell.

Acknowledgemen

Thanks to the Department of Applied Sciences for their help and support.

Conflict of Interest

The authors declare that they have no conflict of interest.

References

[1] S. Zhuk, A. Kushwaha, T. K. S. Wong, S. Masudy-Panah, A. Smirnov, and G. K. Dalapati, "Critical review on sputter-deposited Cu_2ZnSnS_4 (CZTS) based thin film photovoltaic technology focusing on device architecture and absorber quality on the solar cells performance," *Sol. Energy Mater. Sol. Cells*, vol. 171, p. 239–252, 2017.

[2] M. P. Suryawanshi, G.L. Agawane, S.M. Bhosale, S.W. Shin, P.S. Patil, J.H. Kim, et al., "CZTS based thin film solar cells: A status review," *Mater. Technol.*, p. 98–109, 2013.

[3] F. Goumrhar, L. Bahmad, O. Mounkachi, and A. Benyoussef, "Magnetic properties of vanadium doped CdTe: Ab initio calculations," *J. Magn. Magn. Mater.*, vol. 428, p. 368–371, 2017.

[4] F. Goumrhar, L. Bahmad, O. Mounkachi, and A. Benyoussef, "Calculated magnetic properties of co-doped CdTe(V, P): First-principles calculations," Comput. Condens. Matter, vol. 13, p. 87–90, 2017.

[5] S. Rondiya, A. Rokade, A.Jadhavar, S.Nair, M. Chaudhari, R. Kulkarni, et al. , "Effect of calcination temperature on the properties of CZTS absorber layer prepared by RF sputtering for solar cell applications," *Mater. Renew. Sustain. Energy*, vol. 6, p. 1-10, 2017.

[6] A. A. Raiss, Y. Sbai, L. Bahmad, and A. Benyoussef, "Magnetic and Magneto-optical properties of doped and co- doped CdTe with (Mn , Fe): Ab-initio study," *J. Magn. Magn. Mater.*, vol. 385, p.295-301. 2015.

[7] S. Idrissi, H. Labrim, L. Bahmad, and A. Benyoussef, "Structural , Electronic , and Magnetic Properties of the Rare Earth-Based Solar Perovskites: $GdAlO_3$, $DyAlO_3$, and $HoAlO_3$," *J. Supercond. Nov. Magn.*, vol. 3٤, p. 2371-2380, 2021.

[8] A. Ali, J. Jacob, A. Ashfaq, M. Tamseel, K. Mahmood, N. Amin, et al. , "Modulation of structural, optical and thermoelectric properties of sol-gel grown CZTS thin films by controlling the concentration of zinc," *Ceram. Int.*, vol. 45, p. 12820–12824, 2019.

[9] A. G. Kannan, T. E. Manjulavalli, and J. Chandrasekaran, "Influence of Solvent on the Properties of CZTS Nanoparticles," *Procedia Eng.*, vol. 141, pp. 15–22, 2016.

[10] S. S. Patil, S. N. Nadaf, S. S. Mali, C. K. Hong, and P. N. Bhosale, "Optoelectronic and Photovoltaic Properties of the Cu_2ZnSnS_4 Photocathode by a Temperature-Dependent Facile Hydrothermal Route," *Ind. Eng. Chem. Res.*, vol. 60, p. 7816–7825, 2021.

[11] S. S. Patil, R. M. Mane, S. S. Mali, C. K. Hong, and P. N. Bhosale, "Facile designing and assessment of photovoltaic performance of hydrothermally grown kesterite Cu_2ZnSnS_4 thin films: Influence of deposition time," *Sol. Energy*, vol. 201, p. 102–115, 2020.

[12] R. J. Deokate, R. S. Kate, and S. C. Bulakhe, "Physical and optical properties of sprayed Cu 2 ZnSnS 4 (CZTS) thin film: effect of Cu concentration," *J. Mater. Sci. Mater. Electron.*, vol. 30, p. 3530–3538, 2019.

[13] N. A. Yousif, S.M. H. AL-Jawad, and A. A. Taha, "Synthesis and characterization of uncoated and coated magnetite nanoparticles and use of their peroxidase like activity for phenol detection," *Optical and Quantum Electronics*, vol.55, p.1294, 2023.

[14] V. A. Tikkiwal, P. Kwatra, S. V. Singh, D. Chandola, and H. Gandhoke, "A review on sputter deposited CZTS based thin film solar cells," Int. Conf. Comput. Power Commun. Technol. GUCON, pp. 400–404, 2018.

[15] S. M. H. AL-Jawad, N. J. Imran, and K. H. Aboud, "Synthesis and characterization of Mn:CdS nanoflower thin films prepared by hydrothermal method for photocatalytic activity," *J. Sol-Gel Sci. Technol.*, vol. 100, p. 423–439, 2021.

[16] S. M. H. Al-Jawad, O. N. Salman, and N. A. Yousif, "influence of growth time on structural, opticle and electrical properties of TiO_2 nanoroad arrays deposited by hydrothermal method," *Surf. Rev. Lett.*, vol. 26, p. 1–9, 2019.

[17] C. S. A. Raj, S. Sebastian, and S. Rajendran, "A review on Spray pyrolysis deposited CZTS thin films for solar cell applications," *J. Univ. Shanghai Sci. Technol.*, vol. 23, p. 1196–1206, 2021.

[18] S. A. Vanalakar, S. A. Agawane, G. L. Shin, S. W. Suryawanshi, M. P. Gurav, K. V. Jeon, et al.,"A review on pulsed laser deposited CZTS thin films for solar cell applications," *J. Alloys Compd.*, vol. 619, pp. 109–121, 2015.

[19] A. Khare, B. Himmetoglu, M. Johnson, D. J. Norris, M. Cococcioni, and E. S. Aydil, "Calculation of the lattice dynamics and Raman spectra of copper zinc tin chalcogenides and comparison to experiments," *J. Appl. Phys.*, vol. 111, 2012.

[20] S. Schorr, "Structural aspects of adamantine like multinary chalcogenides," *Thin Solid Films*, vol. 515, no. 15, pp. 5985–5991, 2007.

[21] J. He, L. Sun, S. Chen, Y. Chen, P. Yang, and J. Chu, "Composition dependence of structure and optical properties of $Cu_2ZnSn(S,Se)_4$ solid solutions: An experimental study," *J. Alloys Compd.*, vol. 511, p. 129–132, 2012.

[22] M. Handwerg, R. Mitdank, S. Levcenco, S. Schorr, and S. F. Fischer, "Thermal and electrical conductivity of single crystalline kesterite Cu_2ZnSnS_4," *Mater. Res. Express*, vol. 7, p. 105908, 2020.

[23] K. Byrappa and Masahiro Yoshimura, "Hydrothermal technology-principles and applications," 1st, ed., William Andrew,2001.

[24] M. H. Marzbali, S. Kundu, P. Halder, S. Patel, B. G. Hakeem, J. Paz-Ferreiro, et al., "Wet organic waste treatment via hydrothermal processing: A critical review," *Chemosphere*, vol. 279, p. 130557, 2021.

[25] S. M. H. Al-Jawad, M. M. Ismail, and S. F. Ghazi, "Characteristics of diluted magnetic semiconductor based on Mn-doped TiO_2 nanorod array films," *J. Solid State Electrochem.*, vol. 25, p. 435–443, 2021.

[26]H. K. Judran, N. A. Yousif, and S. M. H. AL-Jawad, "Preparation and characterization of CdS prepared by hydrothermal methodQ," *J. Sol-Gel Sci. Technol.*, vol. 97, p. 48–62, 2021.

[27] T. T. Quynh Hoa, L. Van Vu, T. D. Canh, and N. N. Long, "Preparation of ZnS nanoparticles by hydrothermal method," *Journal of Physics: Conference Series*, vol. 187, p. 012081, 2009.

[28] L. Wang, L. Chen, T. Luo, and Y. Qian, "A hydrothermal method to prepare the spherical ZnS and flower-like CdS microcrystallites Licheng," *Mater. Lett.*, vol. 60, p. 3627–3630, 2006.

[29] N. Yousif, S. Al-Jawad, A. Taha, and H. Stamatis, "A review of Structure, Properties, and Chemical Synthesis of Magnetite Nanoparticles," J. Appl. Sci. Nanotechnol., vol. 3, p. 18–31, 2023.

[30] H. Abid, A. Al-Keisy, D. Ahmed, and S. Singh, "Preparation and Characterization of Bi_2MO_6 (M = Mo, W) for Antibacterial Activity," *J. Appl. Sci. Nanotechnol.*, vol. 3, p. 32–40, 2023.

[31] A. Jasim and O. Salman, "The Effect of Solvent Variation on Structural, Optical, and Electrical Properties of TiO_2 Films Prepared by Hydrothermal Method," *J. Appl. Sci. Nanotechnol.*, vol. 3, p. 59–69, 2023.

[32] B. P. Kafle "Chemical analysis and material characterization by spectrophotometry," 1st, ed., Elsevier,2019.

[33] S.H. Feng and G.H.Li , "Hydrothermal and solvothermal syntheses," 2st, ed., Elsevier,2017.

[34] R. F. Mikalsen, "Hydrothermal synthesis of materials for intermediate band solar CELLAS," Ph.D., Department of Chemistry, Norway, 2013.

[35] K. Byrappa and T. Adschiri, "Hydrothermal technology for nanotechnology," *Progress in crystal growth and characterization of materials*, vol. 53, pp. 117–166, 2007.

[36] B. Averill and P. Eldredge, "Chemistry: Principles, pattern, and application," 1st, ed., Pearson Benjamin Cummings,2017.

[37] M. Shandilya, R. Rai, and J. Singh, "Review: Hydrothermal technology for smart materials," *Adv. Appl. Ceram.*, vol. 115, p. 354–376, 2016.

[38] K. Sue, M. Suzuki,K. Arai, T. Ohashi,H. Ura, K. Matsui, et al.,"Size-controlled synthesis of metal oxide nanoparticles with a flow-through supercritical water method," *Green Chem.*, vol. 8, p. 634–638, 2006.

[39] S. M. H. Al-Jawad, O. N. Salman, and N. A. Yousif, "Influence of growth time on structural, optical and electrical properties of TiO_2 nanorod arrays deposited by hydrothermal method," *Surf. Rev. Lett.*, vol. 26, p. 1850155 , 2019.

[40] M. M. Muhsen, S. M. H. Al jawad, and J. Ali, "Gum Arabic - modified Mn - doped CuS nanoprisms for cancer photothermal treatment," *Chem. Pap.*, vol. 76, p. 6821-6838, 2022.

[41] E. L. Shock and H. C. Helgeson, "Calculation of the thermodynamic and transport properties of aqueous species at high pressures and temperatures: Standard partial molal properties of organic species," *Geochim. Cosmochim. Acta*, vol. 54, p. 915–945, 1990.

[42] J.Li,Q.Wu, and, J.Wu," Handbook of Nanoparticles," 1st, ed., Springer, Cham,2015.

[43] S. S. Patil, K. V. Khot, R. M. Mane, and P. N. Bhosale, "Novel hydrothermal route for synthesis of photoactive $Cu_2ZnSn(S,Se)_4$ nanocrystalline thin film: efficient photovoltaic performance," *J. Mater. Sci. Mater. Electron.*, vol. 31, p. 5441–5451, 2020.

[44] K. V. Khot, S. S. Mali, V. B. Ghanwat, S.D. Kharade, R. M. Mane, et al., "Photocurrent enhancement in a $Cu_2Cd(SSe)_2$ photoanode synthesized via an arrested precipitation route," *New J. Chem.*, vol. 40, p. 3277–3288, 2016.

[45] M. Serhan, K.V. Khot, S.H. Sahare, P.N. Bhosale, and T. Bhave, "Low temperature and controlled synthesis of $Bi_2(S_{1-x}Se_x)_3$ thin films using simple chemical route: Effect of bath composition," *RSC Advances*, vol.5, p.57090-57100, 2019.

[46] T. S. Bhat, A. S. Kalekar, D. S. Dalavi, C. C. Revadekar, A. C. Khot, T. D. Dongale , et al.,"Hydrothermal synthesis of nanoporous lead selenide thin films: photoelectrochemical and resistive switching memory applications," *J. Mater. Sci. Mater. Electron.*, vol. 30, p. 17725–17734, 2019.

[47] J. Wang, P. Zhang, X. Song, and L. Gao, "Surfactant-free hydrothermal synthesis of Cu_2ZnSnS_4 (CZTS) nanocrystals with photocatalytic properties," *RSC advances*, vol. 4, p. 27805-27810, 2014.

[48] S. Verma, V. Agrawal, K. Jain, R. Pasricha, and S. Chand, "Green Synthesis of Nanocrystalline Cu_2ZnSnS_4 Powder Using Hydrothermal Route," vol. 2013, 2013.

[49] Shanlong C., H.Tao, Y. Shen, L. Zhu, X. Zeng, J. Tao, et al. , "Facile synthesis of single crystalline sub-micron Cu_2ZnSnS_4 (CZTS) powders using solvothermal treatment," *RSC Advances* , vol.5, p.6682-6686,2015.

[50] S. Gokhan, C. V. Sezer ,R. E. Demirdogen, M. Ince, F. M. Emen, K. Ocakoglu, et al., "Investigation of in vitro activities of Cu_2 $ZnSnS_4$ nanoparticles in human non-small cell lung cancer," *Mater. Today Commun.*, vol. 27, p. 102304, 2021.

[51] S. Das, K. Sa, P. C. Mahakul, J Raiguru, I Alam, BVRS Subramanyam, et al., "Synthesis of quaternary chalcogenide CZTS nanoparticles by a hydrothermal route," *IOP Conf. Ser. Mater. Sci. Eng.*, vol. 338, p. 012062 , 2018.

[52] K. Maurya, S. Sikarwar, P. Chaudhary, S. Angaiah, and B. C. Yadav, "Synthesis and Characterization of Nanostructured Copper Zinc Tin Sulphide (CZTS) for Humidity Sensing Applications," *IEEE Sens. J.*, vol. 19, p. 2837–2846, 2019.

[53] S. S. Mali, H. Kim, C. S. Shim, P. S. Patil, and C. K. Hong,"Polyvinylpyrrolidone (PVP) assisted single-step synthesis of kesterite Cu_2ZnSnS_4 nanoparticles by solvothermal process," *Phys. Status Solidi - Rapid Res. Lett.*, vol. 7, p. 1050–1054, 2013.

[54] Z. Syum, T. Billo, A. Sabbah, B. Venugopal, S. Yu, F. Fu, et al., "Copper Zinc Tin Sul fi de Anode Materials for Lithium-Ion Batteries at Low Temperature," vol. 9, p. 8970–8979, 2021.

[55] S. A. Phaltane, S. A. Vanalakar, T. S. Bhat, P. S. Patil, S. D. Sartale, and L. D. Kadam, "Photocatalytic degradation of methylene blue by hydrothermally synthesized CZTS nanoparticles," *J. Mater. Sci. Mater. Electron.*, vol. 28, p. 8186–8191, 2017.

[56] X. Gu,S. Zhang, Y. Qiang,Y. Zhao, and L. Zhu, "Synthesis of Cu_2ZnSnS_4 Nanoparticles for Applications as Counter Electrodes Synthesis of Cu_2ZnSnS_4 Nanoparticles for Applications as Counter Electrodes of CdS Quantum Dot-Sensitized Solar Cells," *Journal of electronic materials*, vol. 43, p. 2709-2714, 2014.

[57] M. Karbassi, S. Baghshahi, N. Riahi-Noori, and R. S. Moakharc, "Synthesis of Cu_2ZnSnS_4 (CZTS) Ink by an Easy Hydrothermal Method,"*Research Square*, vol. 4, 2021.

[58] V. Patil, V. L. Patil, P. S. Patil, and J. H. Kim, "Controllable synthesis of stoichiometric Cu_2ZnSnS_4 nanoparticles by solvothermal method and its properties," In AIP Conference Proceedings, vol. 1665, 2016.

[59] D.L. S. Pinzónand, R. De Janeiro, and J.A. G. Cuaspud,"Hydrothermal Synthesis and Evaluation of the Cu_2ZnSnS_4 for Photovoltaic Applications," *Mater. Res.*, vol. 24, 2021.

[60] K. Tikote, M. A. More, N. B. Chaure, E. V. López, and M. Schmala "Polycrystalline and stoichiometric growth of CZTS by hydrothermal method Polycrystalline and stoichiometric growth of CZTS by hydrothermal method," AIP Conference Proceedings, vol. 030669, 2020.

[61] H. Zheng, A. Wei, and H. Xiong, "Influence of deposition parameters on the morphology, structural and optical properties of Cu_2ZnSnS_4 thin films grown by solvothermal method," *Chalcogenide Lett.*, vol. 15, p. 327–337, 2018.

[62] S. Shen, J. Shi, P. Guo, and L. Guo. "Visible-light-driven photocatalytic water splitting on nanostructured semiconducting materials," I*nternational Journal of Nanotechnology*, vol. 8, p.523-591, 2012.

[63] X. Zhai, H. Jia, Y.Zhang, Y. Lei, J. Wei, Y. Gao, et al., "In situ fabrication of Cu_2ZnSnS_4 nanoflake thin films on both rigid and flexible substrates," *CrystEngComm*, vol.16, p. 6244-6249, 2014.

[64] Y. Huang, G. Li, Q. Fan, M. Zhang, Q. Lan, X. Fan, et al., "Facile solution deposition of Cu_2 $ZnSnS_4$ (CZTS) nano-worm films on FTO substrates and its photoelectrochemical property," *Appl. Surf. Sci.*, vol. 364, pp. 148–155, 2016.

[65] Z. Shadrokh, A. Yazdani, and H. Eshghi, "Study on Structural and Optical Properties of Wurtzite Cu_2ZnSnS_4 Nanocrystals Synthesized via Solvothermal Method," *International Journal of Nanoscience and Nanotechnology* , vol.13, p. 359-366, 2017.

[66] V. T. Tiong, T. Hreid, G. Will, J. Bell, and H. Wang,"Polyacrylic acid assisted synthesis of Cu_2ZnSnS_4 by hydrothermal method," *Sci. Adv. Mater.*, vol. 6, p. 1467–1474, 2014.

[67] K. Mohammed, K. U. Isah, U. E. Uno, A. Mann, and N. Nayan, "Influence of Hydrothermal Synthesis Reaction Duration on the Properties of Cu_2ZnSnS_4 (CZTS) Thin Films," I*nternational Journal of Current Engineering and Technology*, vol.9, 2019.

[68] S. Sarkar, K. Bhattacharjee, G. C. Das, and K. K. Chattopadhyay, "Self-sacrificial template directed hydrothermal route to kesterite-Cu_2ZnSnS_4 microspheres and study of their photo response properties," *CrystEngComm*, vol 16, p. 2634-2644, 2014.

[69] C. Wang, C. Cheng, Y. Cao, W. Fang, L. Zhao, and X. Xu, "Synthesis of Cu_2ZnSnS_4 nanocrystallines by

a hydrothermal route," *Jpn. J. Appl. Phys.*, vol. 50, p. 28–30, 2011.
[70]J. D. Cristóbal-García, F. Paraguay-Delgado, G. Herrera-Pérez, R. Y. Sato-Berrú, and N. R. Mathews, "Polyvinylpyrrolidone influence on physical properties of Cu_2ZnSnS_4 nanoparticles," *J. Mater. Sci. Mater. Electron.*, vol. 29, p. 20302–20311, 2018.
[71]Y. Al-hadeethi, E. M. Mkawi, O. Al-hartomy, and E. Bekyarova, "Solvothermal synthesis of kesterite Cu_2ZnSnS_4 nanocrystals : Influence of glycine complexing agent concentration on properties," *Ceram. Int.*, vol. 47, p. 11568–11573, 2021.
[72] F. Liang, J. Gao, C. Zou, and L. Shao, "Cu_2ZnSnS_4 Nanoparticles Synthesized by a Novel Diethylenetriamine-Assisted Hydrothermal Method," *J. Korean Phys. Soc.*, vol. 72, p. 1033–1038, 2018.
[73] A. Wei, Z. Yan, Y. Zhao, M. Zhuang, and J. Liu, "Solvothermal synthesis of Cu_2ZnSnS_4 nanocrystalline thin films for application of solar cells," I*nt. J. Hydrogen Energy*, vol. 40, p. 797–805, 2015.
[74] S. WookáShin, W. RiáBae, H. SeungáYang, C. WooáHong, H. RimáJung, J. YongáLee, et al., "Size and shape controlled hydrothermal synthesis of kesterite Cu_2ZnSnS_4 nanocrystals," *RSC Advances*, vol.4, p. 32530-32533, 2014.
[75] E. M. Mkawi, Y. Al-hadeethi, E. Shalaan, and E. Bekyarova, "Fabricating chalcogenide Cu_2ZnSnS_4 (CZTS) nanoparticles via solvothermal synthesis : E ff ect of the sulfur source on the properties," *Ceram. Int.*, vol. 4٦, p. 24916-24922, 2020.
[76] S. Lin, J. Ting, and Y. Fu,"Single-phase , high-purity Cu_2ZnSnS_4 nanoparticles via a hydrothermal route," *Ceram. Int.*, vol. 44, p. 4450-4456, 2018.
[77] T. V. Tiong, Y. Zhang, J. Bell, and H. Wang, "Phase-selective hydrothermal synthesis of Cu_2ZnSnS_4 nanocrystals: the effect of the sulphur precursor," *CrystEngComm* , vol.16, p.4306-4313, 2014.
[78]M. Suryawanshi,S. W. Shin,W. R. Bae,K. Gurav, M. G. Kang,G. Agawane, et al., "Kesterite CZTS nanocrystals: PH-dependent synthesis," *Phys. Status Solidi Appl. Mater. Sci.*, vol. 211, p. 1531–1534, 2014.
[79] S. A. Vanalakar, A.S. Kamblea, S.W. Shina, S.S. Malid, G.L. Agawanea, V.L. Patil, et al., "Simplistic toxic to non-toxic hydrothermal route to synthesize Cu_2ZnSnS_4 nanoparticles for solar cell applications," *Sol. Energy*, vol. 122, p. 1146–1153, 2015.
[80] C. Zhang, F. Yue, and Y. Shi, "Morphology dependence of performance of counter electrodes for dye-sensitized solar cells of hydrothermally prepared hierarchical Cu2ZnSnS4 nanostructures," pp. 2–7, 2018.
[81] S. M. Camara, L. Wang, and X. Zhang, "Easy hydrothermal preparation of Cu_2ZnSnS_4 (CZTS) nanoparticles for solar cell application," *Nanotechnology*, vol. 24, p. 495401, 2013.
[82]Y. Huang , G. Li,Q. Fan,M. Zhang, Q.Lan,X. Fan,et al., "Facile solution deposition of Cu_2ZnSnS_4 (CZTS) nano-worm films on FTO substrates and its photoelectrochemical property," *Appl. Surf. Sci.*, vol. 364, p. 148–155, 2016.
[83] S. J. Lin, J. M. Ting, C. T. Hung, and Y. S. Fu, "Effect of the vapor diffusion and improved light harvesting for Perovskite-Cu_2ZnSnS_4 hybridized solar cells," *Org. Electron.*, vol. 59, p. 190–195, 2018.
[84] S. S. Patil, S. N. Nadaf, S. S. Mali, C. K. Hong, and P. N. Bhosale, "Optoelectronic and Photovoltaic Properties of the Cu_2ZnSnS_4 Photocathode by a Temperature-Dependent Facile Hydrothermal Route," *Ind. Eng. Chem. Res.*, vol. 60, p. 7816–7825, 2021.
[85] J. P. Sawant and R. B. Kale, "Surfactant mediated TiO_2 photoanodes and Cu_2ZnSnS_4 counter electrodes for high efficient dye sensitized solar cells," *Mater. Lett.*, vol. 265, p. 127407, 2020.
[86]J. P. Sawant and R. B. Kale, "CZTS counter electrode in dye-sensitized solar cell: enhancement in photo conversion efficiency with morphology of TiO_2 nanostructured thin films," *J. Solid State Electrochem.*, vol. 24, p. 461–472, 2020.
[87] J. P. Sawant, R. Rajput, S. Patil, J. Ryu, D. R. Patil, and R. B. Kale, "Photocatalytic activities of hydrothermal synthesized copper zinc tin sulfide nanostructures," *J. Mater. Sci. Mater. Electron.*, vol. 32, p. 22803–22812, 2021.
[88] M. M. S. Sanad, A. M. Elseman, M. M. Elsenety, M. M. Rashad, and B. A. Elsayed, "Facile synthesis of sulfide-based chalcogenide as hole-transporting materials for cost-effective efficient perovskite solar cells," *J. Mater. Sci. Mater. Electron.*, vol. 30, p. 6868–6875, 2019.
[89] Y. Li, M. Yang, Y. Huang, X. Sun, K. Liu, and J. Zhang, "In situ solvothermal growth of Cu_2ZnSnS_4 thin film for counter electrode of dye-sensitized solar cells," *Solid State Sci.*, vol. 113, p. 106547, 2021.
[90]K. Pal, P. Singh, A. Bhaduri, and K. B. Thapa, "Current challenges and future prospects for a highly efficient (>20%) kesterite CZTS solar cell: A review," *Sol. Energy Mater. Sol. Cells*, vol. 196, p. 138–156, 2019.
[91] M. F. Islam, N. M. Yatim, and M. A. H. Ismail, "A Review of CZTS Thin Film Solar Cell Technology," *J.*

Adv. Res. Fluid Mech. Therm. Sci., vol. 81, p. 73–87, 2021.

[92] M. Ravindiran and C. Praveenkumar, "Status review and the future prospects of CZTS based solar cell – A novel approach on the device structure and material modeling for CZTS based photovoltaic device," *Renew. Sustain. Energy Rev.*, vol. 94, , p. 317–329, 2018.